4D-CT scans reveal reduced magnitude of respiratory liver motion achieved by different abdominal compression plate positions in patients with intrahepatic tumors undergoing helical tomotherapy

Yong Hu,[a] Yong-Kang Zhou,[b] Yi-Xing Chen,[c] Shi-Ming Shi,[d] and Zhao-Chong Zeng[e]
Department of Radiation Oncology, Zhongshan Hospital, Fudan University, 180 Feng Lin Road, Shanghai 200032, China

(Received 3 February 2016; revised 18 May 2016; accepted for publication 19 May 2016; published 21 June 2016)

Purpose: While abdominal compression (AC) can be used to reduce respiratory liver motion in patients receiving helical tomotherapy for hepatocellular carcinoma, the nature and extent of this effect is not well described. The purpose of this study was to evaluate the changes in magnitude of three-dimensional liver motion with abdominal compression using four-dimensional (4D) computed tomography (CT) images of several plate positions.
Methods: From January 2012 to October 2015, 72 patients with intrahepatic carcinoma and divided into four groups underwent 4D-CT scans to assess respiratory liver motion. Of the 72 patients, 19 underwent abdominal compression of the cephalic area between the subxiphoid and umbilicus (group A), 16 underwent abdominal compression of the caudal region between the subxiphoid area and the umbilicus (group B), 11 patients underwent abdominal compression of the caudal umbilicus (group C), and 26 patients remained free breathing (group D). 4D-CT images were sorted into ten-image series, according to the respiratory phase from the end inspiration to the end expiration, and then transferred to treatment planning software. All liver contours were drawn by a single physician and confirmed by a second physician. Liver relative coordinates were automatically generated to calculate the liver respiratory motion in different axial directions to compile the 10 ten contours into a single composite image. Differences in respiratory liver motion were assessed with a one-way analysis of variance test of significance.
Results: The average respiratory liver motion in the Y axial direction was 4.53 ± 1.16, 7.56 ± 1.30, 9.95 ± 2.32, and 9.53 ± 2.62 mm in groups A, B, C, and D, respectively, with a significant change among the four groups ($p < 0.001$). Abdominal compression was most effective in group A (compression plate on the subxiphoid area), with liver displacement being 2.53 ± 0.93, 4.53 ± 1.16, and 2.14 ± 0.92 mm on the X-, Y-, and Z-axes, respectively. There was no significant difference in respiratory liver motion between group C (displacement: 3.23 ± 1.47, 9.95 ± 2.32, and 2.92 ± 1.10 mm on the X-, Y-, and Z-axes, respectively) and group D (displacement: 3.35 ± 1.55, 9.53 ± 2.62, and 3.35 ± 1.73 mm on the X-, Y-, and Z-axes, respectively). Abdominal compression was least effective in group C (compression on caudal umbilicus), with liver motion in this group similar to that of free-breathing patients (group D).
Conclusions: 4D-CT scans revealed significant liver motion control via abdominal compression of the subxiphoid area; however, this control of liver motion was not observed with compression of the caudal umbilicus. The authors, therefore, recommend compression of the subxiphoid area in patients undergoing external radiotherapy for intrahepatic carcinoma. [http://dx.doi.org/10.1118/1.4953190]

Key words: four-dimensional CT, abdominal compression, intrahepatic tumor, respiratory liver motion

1. INTRODUCTION

With current advancements in precision radiotherapy, patient immobilization, target positioning, and control of organ motion continue to be critical for treatment success in complex cases involving higher doses of radiation. Respiration-induced liver motion (i.e., respiratory liver motion) is anisotropic, occurring primarily in the cephalic-caudal direction and reaching a range of motion from 5 to 50 mm.[1,2] Therefore, it is imperative to manage and/or account for respiratory liver motion through means such as abdominal compression (AC),[3–5] which uses a constant force applied to the abdomen to reduce liver motion, respiratory gating techniques[6–8] to deliver radiation only to the tumor during the respiratory cycle, and active breathing control,[9,10] which achieves temporary and reproducible inhibition of respiration-induced motion by monitoring the patient's breathing cycle and implementing a breath hold at a predefined stage of respiration and air flow direction. The Body Pro-Lok™ system[11] is an easy-to-use modular structure that can facilitate the administration

of complex stereotactic body radiotherapy through AC by bridging a respiratory belt and plate and thus providing a number of options to help control the amount of liver motion resulting from patient breathing. AC can significantly reduce three-dimensional (3D) liver tumor motion in most patients and has been widely used to reduce liver motion during both radiotherapy and radiodiagnosis.[3,4] Varying forces on the abdomen may inhibit liver motion to different degrees; for example, using four-dimensional (4D) computed tomography (CT), Heinzerling *et al.*[12] demonstrated significantly improved control of liver tumor motion with strong abdominal compression compared to medium abdominal compression.

Abdominal compression is commonly used for reducing thoracic or abdominal tumor motion during radiation therapy;[12,13] however, the effects of various abdominal compression plate positions have never been described. In this study, we used 4D-CT scans to investigate the magnitude of the reduction of respiration-induced liver motion achieved by different abdominal compression plate positions in patients with intrahepatic tumors undergoing helical tomotherapy.

2. MATERIALS AND METHODS

2.A. Patients

Patient demographics and clinical characteristics are shown in Table I. Between January 2012 and October 2015, 72 consecutive patients (59 males, 13 females; age range 23–88 yr; no disease affecting cardio-pulmonary function) diagnosed with intrahepatic carcinoma were divided into four groups (described in more detail below) and underwent 4D-CT scans to assess respiratory liver motion. All patients had Child-Pugh Class A liver function and a Karnofsky performance status of >80. Patients with colostomy and ascites were excluded from the study. Each patient's breathing rate was kept regular through a training session under AC. The study was approved by the Ethics Committee of Zhongshan Hospital, Fudan University (Ethics Approval No: 2011-235). Informed consent was obtained from all patients.

2.B. Abdominal compression

Patients were divided into groups A, B, C, and D based on the plate positioning of abdominal compression (Fig. 1). Abdominal compression on the cephalic area between the subxiphoid and umbilicus was applied to 19 patients (group A), abdominal compression on the caudal area between the subxiphoid and the umbilicus was applied to 16 patients (group B), abdominal compression on the caudal umbilicus was applied to 11 patients (group C), and 26 patients did not receive abdominal compression but remained free breathing (group D). Each patient underwent a basic respiratory training guided by a radiotherapy oncologist and therapist before administration of AC. AC was applied during each patient's end expiration until maximum tolerability was reached, as indicated by the patient. In this study, we found that abdominal breathing clearly switched to thoracic breathing with satisfactory abdominal compression, especially in male patients.

TABLE I. Patient demographics and clinical characteristics.

	Group A ($n = 19$)	Group B ($n = 16$)	Group C ($n = 11$)	Group D ($n = 26$)	p-value
Sex, n (%)					0.774
Male	16(84.2)	13(81.3)	10(90.9)	20(76.9)	
Female	3(15.8)	3(18.7)	1(9.1)	6(23.1)	
Age, n (%)					0.356
≤60 years old	13(68.4)	12(75.0)	5(45.5)	19(73.1)	
>60 years old	6(31.6)	4(25.0)	6(54.5)	7(26.9)	
Intrahepatic lesions, n (%)					0.984
Solitary	11(57.9)	9(56.3)	7(63.6)	15(57.7)	
Multiple nodules	8(42.1)	7(43.7)	4(36.4)	11(42.3)	
Diameter, n (%)					0.953
≤5 cm	11(57.9)	10(62.5)	6(54.5)	14(53.8)	
>5 cm	8(42.1)	6(37.5)	5(45.5)	12(46.2)	
TACE, n (%)					0.492
Yes	14(73.7)	14(87.5)	7(63.6)	18(69.2)	
No	5(26.3)	2(12.5)	4(36.4)	8(30.8)	
Postoperative recidivation, n (%)					0.651
Yes	4(21.1)	5(31.3)	3(27.3)	4(15.4)	
No	15(78.9)	11(68.7)	8(72.7)	22(84.6)	
Height, n (%)					0.588
≤170 cm	11(57.9)	7(43.8)	6(54.5)	17(65.4)	
>170 cm	8(42.1)	9(56.3)	5(45.5)	9(34.6)	
Weight, n (%)					0.258
≤70 kg	14(73.7)	10(62.5)	5(45.5)	20(76.9)	
>70 kg	5(26.3)	6(37.5)	6(54.5)	6(23.1)	

Note: TACE, transarterial chemoembolization.

Each patient was assigned to one of the four groups based on when, during the study period, the patient was enrolled; for the purpose of group assignment, the study period was divided into four stages. In the first stage (January 2012 to February 2013), 26 patients were assigned to group D and underwent therapy in the free-breathing group. In the second stage (March 2013 to November 2013), 11 patients underwent abdominal compression of the caudal umbilicus (group C). During this stage, we were excessively concerned about the effect of the target radiotherapy dose because of the x-ray sheltering by the high-electron density plate for a period of time, especially for those patients with tumors located in the inferior right lobe of the liver. In the third stage (December 2013 to October 2014), 16 patients underwent abdominal compression of the caudal region between the subxiphoid area and the umbilicus (group B). In this stage, we also slightly adjusted compression plate positions in the cranial-caudal direction based on the patients' various intrahepatic tumor localizations; but the compression plate positions were all limited to the caudal region between the subxiphoid area and the umbilicus. In the fourth stage (November 2014 to October 2015), 19 patients underwent abdominal compression of the cephalic area between the subxiphoid and umbilicus (group A).

2.C. 4D-CT image acquisition

4D-CT scans were obtained using a Brilliance Big Bore CT Scanner a CT-simulation scanner (Siemens Somatom CT,

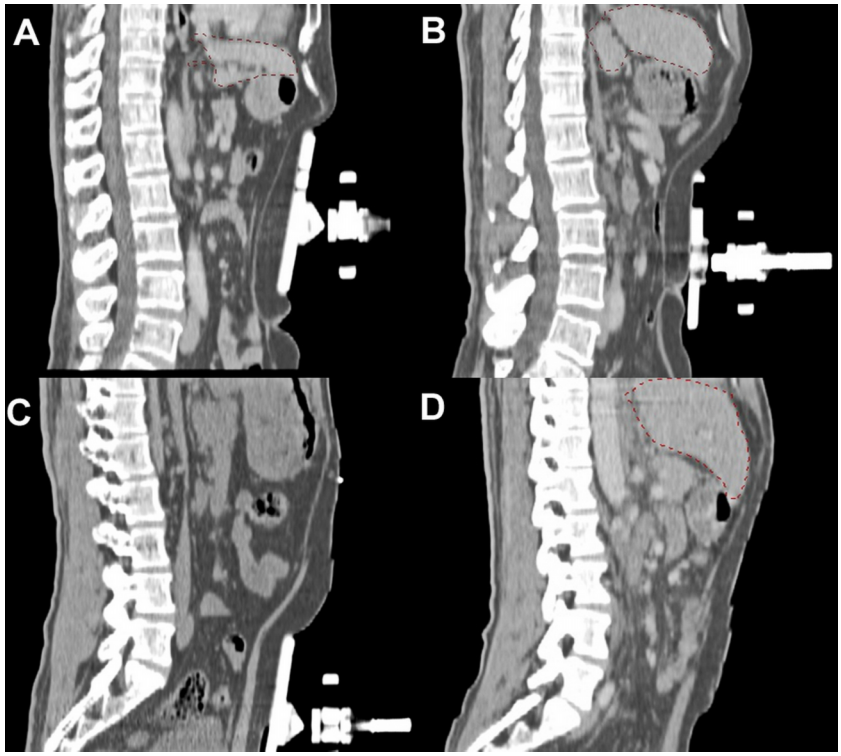

FIG. 1. CT sagittal reconstruction images illustrate respiratory status of each patient group. (A) shows a patient with the compression plate placed on the subxiphoid area (group A), (B) shows a patient with the compression plate placed on the caudal region between the subxiphoid area and umbilicus (group B), (C) shows a patient with the compression plate placed on the caudal umbilicus (group C), and (D) shows a free-breathing patient (group D).

Sensation Open; Siemens Healthcare, Munchen Germany). Patients were placed in a supine position with arms raised above the forehead and were immobilized using a Body Pro-Lok™ system with or without abdominal compression. We used the "Res Low Breath Rate (X-ray tube setting of 120 kV, 400 mAs; Pitch 0.1; Gantry rotation cycle time 1 s; 3 mm reconstructed thickness)" scanning mode when the respiratory cycle of each patient was >5 s, evidence of satisfactory abdominal compression. Patients in groups A, B, and C, which underwent AC, also were 4D-CT scanned. The respiratory phase on the respiratory wave was manually adjusted and confirmed by the CT-simulation technician before CT-image reconstruction. The 4D-CT images from the respiratory raw data were sorted into 10 CT-image series (CT0–CT90) according to the respiratory cycle, with CT0 being defined as the end-inspiration phase and CT50 the end-expiration phase.[14] Datasets for 4D-CT scans were then transferred to Nucletron Oncentra's treatment planning software VERSION 4.3 (NUCLETRON B.V., Veenendaal, Netherlands), and all liver contours were drawn by an experienced observer (HY) and confirmed by a single physician (YKZ).

2.D. Liver displacement acquisition and analysis

Liver contours were delineated at all CT-image phases and then copied manually to a single plan. Nine liver contours of CT10–CT90 were copied onto a CT0 image, which were named $\text{Copy}_{\text{Contour10}}$–$\text{Copy}_{\text{Contour90}}$. There were ten liver contours ($\text{Copy}_{\text{Contour10}}$–$\text{Copy}_{\text{Contour90}}$ and liver contours of CT0) on the CT0 image. Then, 0° and 90° digitally reconstructed radiography beams were added to the CT0 image. Ten liver 3D contours could be projected onto the digitally reconstructed radiography images in the directions of 0° and 90°. Overlays of ten liver contours were shown on the digitally reconstructed radiography images of 0° and 90°. We show the overlays on the 0° digitally reconstructed radiography images for a patient in each group in Fig. 2. The relative coordinates of the liver were automatically generated to calculate the respiratory liver motion in different axial directions. The position for each liver was expressed using the X (left–right; LR), Y (cranial-caudal; CC), and Z (anterior–posterior; AP) coordinates of the center of mass for each 4D-CT bin. Then, the range of respiratory liver motion from the center of mass of each coordinate was obtained. The maximum range of motion in each axial direction was obtained after the maximum relative coordinate value minus the minimum relative coordinate value was calculated. The 3D motion vector of the center of mass was calculated according to the following formula: $V = \left({}_{\Delta}X^2 + {}_{\Delta}Y^2 + {}_{\Delta}Z^2\right)^{1/2}$. Variables were expressed as the mean ± the standard deviation.

2.E. Statistical analyses

A chi-square (χ^2) test was used to compare patient demographics and clinical characteristics between the four patient groups (A–D). The variations between the four groups in the X, Y, Z, and 3D directions were assessed using a one-way analysis of variance test, while a Pearson correlation was used to analyze the relationship between the 3D vectors and the distance of the compression plate from the subxiphoid area

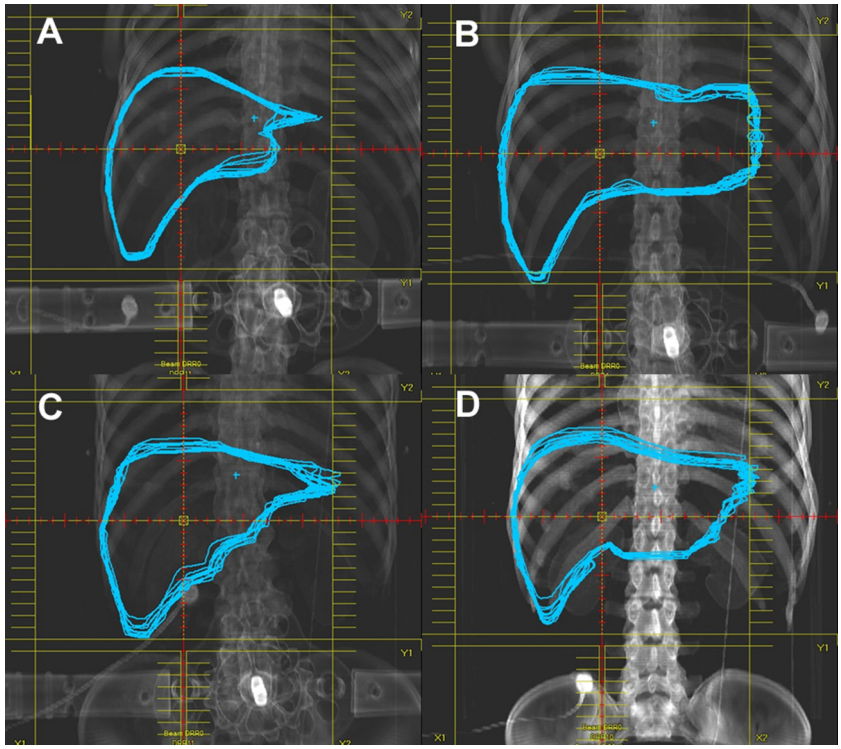

FIG. 2. An overlay of ten liver contours rendered on a digitally reconstructed radiography image shows the effects of various compression strengths [tight to loose from (A) to (D)]. The image in (A) is from a group A patient, the image in (B) is from a group B patient, the image in (C) is from a group C patient, and the image in (D) is from a group D patient.

(DTS). The significance cutoff was $p < 0.05$. All calculations were performed using SPSS 15.0 for Windows (Chicago, IL, USA).

3. RESULTS

3.A. Respiratory liver motion

Table II lists the respiratory liver motion in the relative X, Y, Z, and 3D axial directions for each patient group (A–D). Respiratory liver motion was anisotropic, and differences were manifested in all axial directions in four respiration states (see Table II and Fig. 2), especially in the Y axial direction. The average liver respiratory motion in the Y axial direction was 4.53 ± 1.16, 7.56 ± 1.30, 9.95 ± 2.32, and 9.53 ± 2.62 mm in groups A, B, C, and D, respectively, with a significant difference in respiratory liver motion among the four groups ($p < 0.001$). Abdominal compression was most effective in group A (the compression plate on the subxiphoid area), with an X-, Y-, and Z-axes displacement of 2.53 ± 0.93, 4.53 ± 1.16, and 2.14 ± 0.92 mm, respectively. Abdominal compression was least effective in group C (compression plate on the caudal umbilicus), which had a respiratory liver motion similar to that of group D (control group; free-breathing). There was no significant difference in respiratory liver motion between group C (X-, Y-, and Z-axes displacement of 3.23 ± 1.47, 9.95 ± 2.32, and 2.92 ± 1.10 mm, respectively) and group D (X-, Y-, and Z-axes displacement of 3.35 ± 1.55, 9.53 ± 2.62, and 3.35 ± 1.73 mm, respectively).

TABLE II. The magnitude of respiratory liver motion (mm) in different axial directions among the four patient groups is illustrated. Data are presented as the mean ± standard deviation.

	X-axis	Y-axis	Z-axis	3D
Group A ($n = 19$)	2.53 ± 0.93	4.53 ± 1.16	2.14 ± 0.92	5.81 ± 0.84
Group B ($n = 16$)	2.18 ± 0.72	7.56 ± 1.30	2.78 ± 1.41	8.50 ± 1.22
Group C ($n = 11$)	3.23 ± 1.47	9.95 ± 2.32	2.92 ± 1.10	10.99 ± 2.42
Group D ($n = 26$)	3.35 ± 1.55	9.53 ± 2.62	3.35 ± 1.73	10.94 ± 2.28
Test statistic (F)	3.73	27.38	2.81	34.40
p-value	0.015	0.000	0.046	0.000

3.B. The distribution of Y-axis displacement in group A patient livers

As shown in Fig. 3, most of the respiratory liver motion was in the range of 3–6 mm (21.05% of patients reached 3–4 mm, 26.32% of patients reached 4–5 mm, and 26.32% of patients reached 5–6 mm). A total of 10.52% of patients experienced reduced liver respiratory motion of 2–3 mm on the Y-axis; however, respiratory liver motion was not reduced to a satisfactory level in all patients, with 15.79% of patients with a liver displacement of >6 mm despite abdominal compression plate placement on the subxiphoid area.

3.C. 3D vectors

The mean 3D motion vector was 5.81 ± 0.84 mm (range 4.31–7.82 mm), 8.50 ± 1.22 mm (range 6.25–10.75 mm),

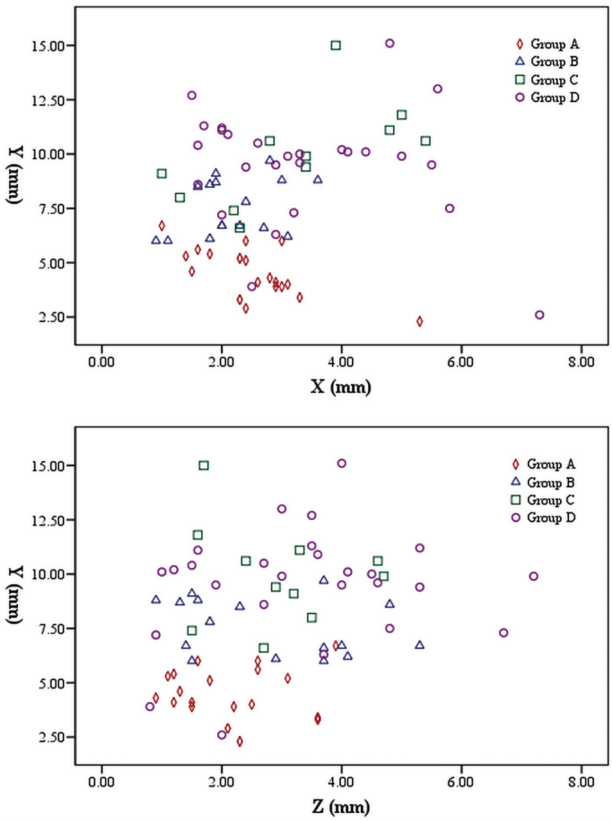

FIG. 3. Scatter plots illustrate the respiratory liver motion in the X, Y, and Z axial directions in the four patient groups.

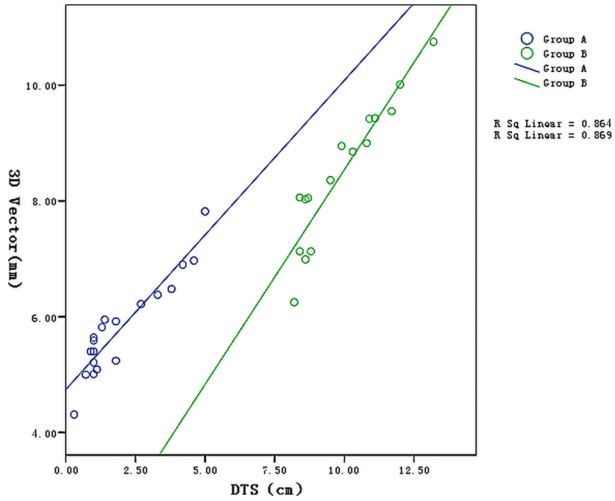

FIG. 4. The relationship between DTS and the 3D liver motion vector in patient groups A and B is illustrated. R^2 values are indicated to the right of the graph. The top R^2 value belongs to group A, and the bottom R^2 value belongs to group B, which show a strong correlation between the 3D vector and the DTS.

10.99 ± 2.42 mm (range 7.49–15.59 mm), and 10.94 ± 2.28 mm (range 4.70–16.34 mm) for groups A, B, C, and D, respectively, with a significant difference between the groups ($F = 34.40$, $p < 0.001$; see Table II). There was a significant correlation between the DTS and the 3D vector ($r = 0.941$, $p < 0.001$) when the compression plate was placed between the subxiphoid area and umbilicus. Additionally, there was a strong correlation between the DTS and the 3D vector in groups A and B ($r = 0.929$, $p < 0.001$ and $r = 0.932$, $p < 0.001$, respectively; see Fig. 4).

4. DISCUSSION

The benefit of abdominal compression in reducing respiratory liver motion is well known. Reduced liver motion via AC can lead to reduced internal target volume (ITV),[15–18] enabling physicians to avoid unnecessary liver parenchyma irradiation and inadequate tumor coverage. An increase in respiratory tumor motion by double corresponds to a nearly eight times increase in intrahepatic tumor ITV. Eccles *et al.*[3] reported that interfraction liver deformations in patients receiving stereotactic body radiation therapy under abdominal compression after rigid liver-to-liver registrations on cone beam CT scans sorted according to respiration cycle were small (<5 mm) in most patients. Similarly, Case *et al.*[2] reported that both inter and intrafraction changes in the amplitude of liver motion under abdominal compression are small (<2 mm) in the direction of the Y-axis. Heinzerling *et al.*[12] reported that mean overall liver tumor motion was 13.6 mm (2 sigma [2 sigma] 11.5–15.6) without compression, 8.3 mm (2 sigma [2 sigma] 6.0–10.5) under medium-compression force, and 7.2 mm (2 sigma [2 sigma] 5.4–9.0) under high-compression force. In our study, we observed an average liver motion distance in the direction of the Y-axis of 4.5 mm when abdominal compression was applied, a larger magnitude than that reported by both Eccles *et al.* and Case *et al.* In our study, the total abdominal compression time experienced by patients was about 25 min, including setup, megavoltage CT, image-guided scan, and treatment.[19] This time is much longer than that of patients in the studies of Eccles *et al.* and Case *et al.*; therefore, the increased AC time experienced by patients in our study is likely responsible for the increased magnitude of liver motion observed in our study compared to others.

In the current study, we did not perform contrast-enhanced (CE) 4D-CT scans. Arterial-phase contrast-enhanced 3D-CT images are commonly used to determine the gross tumor volume boundary, which can help identify the liver tumor boundary. While the application of 4D CT in hepatocellular carcinoma radiotherapy has proven promising clinically, the application of CE 4D-CT scans is lacking due to the difficulty in capturing the timing of contrast agent injection during the extended 4D-CT image acquisition process.[20] Although Beddar *et al.*[21] developed a tumor-specific protocol for 4D-CT imaging of liver tumors using synchronized intravenous contrast injection to improve the accuracy of tumor delineation for treatment planning, only intrahepatic metastases or cholangiocarcinomas can be successfully imaged in the portal venous phase, a phenomenon that we have confirmed. Due to the difficulty in visualizing liver tumors on 4D CT, and because liver contour variation can effectively illustrate the effects of various compression plate positions, we used liver contours other than the intrahepatic tumor in the current study.

In this study, we used a high-electron-density compression plate provided by CIVCO, the use of which may affect the target radiotherapy dose because of the x-ray sheltering by the high-electron-density plate. Various positions of the compression plate were applied on patients with various intrahepatic tumor localizations. To avoid x-ray sheltering by the high-electron-density plate, compression was applied to the lower abdomen caudal umbilicus, especially for those patients with tumors located in the inferior right lobe of the liver. Compared with intensity-modulated radiation therapy, helical tomotherapy is an optimal technique for overcoming the effects of respiration during abdominal tumor radiotherapy.[22,23] All patients in this study have undergone helical tomotherapy.

In theory, abdominal compression may increase the risk of intrahepatic tumor rupture and bleeding, which, however, were not observed in any of the patients in our study. This may be because abdominal compression was applied during each patient's end expiration phase, which may reduce the rigid connection between the compression plate and the patient's abdomen. Abdominal compression was not used in patients with risk of thrombosis or colostomy, as proposed by Eccles *et al.*[3] Dohmen *et al.* described a patient with liver cirrhosis who suffered rapid development of a hydrothorax after manual compression of the abdomen.[24] Thus, in the current study, contraindications for abdominal compression were the risk of thrombosis or colostomy rather than the big tumor size.

5. CONCLUSION

Four-dimensional CT demonstrated that the use of abdominal compression on the subxiphoid area reduced respiration-induced liver motion. The further away from the subxiphoid area the compression was, the greater the magnitude of liver motion; and abdominal compression was completely ineffective when the compression plate was placed on the caudal umbilicus. We, therefore, recommend compression of the subxiphoid area in patients undergoing external radiotherapy for intrahepatic carcinoma.

CONFLICT OF INTEREST DISCLOSURE

The authors have no COI to report.

[a]Electronic mail: hu.yong@zs-hospital.sh.cn
[b]Electronic mail: zhouyk2009@163.com
[c]Electronic mail: chen.yixing@zs-hospital.sh.cn
[d]Electronic mail: shiming32@126.com
[e]Author to whom correspondence should be addressed. Electronic mail: zeng.zhaochong@zs-hospital.sh.cn

[1]J. M. Balter, L. A. Dawson, S. Kazanjian, C. McGinn, K. K. Brock, T. Lawrence, and R. Ten Haken, "Determination of ventilatory liver movement via radiographic evaluation of disphragm position," Int. J. Radiat. Oncol., Biol., Phys. **51**, 267–270 (2001).
[2]R. B. Case, D. J. Moseley, J. J. Sonke, C. L. Eccles, R. E. Dinniwell, J. Kim, A. Bezjak, M. Milosevic, K. K. Brock, and L. A. Dawson, "Interfraction and intrafraction changes in amplitude of breathing motion in stereotactic liver radiotherapy," Int. J. Radiat. Oncol., Biol., Phys. **77**(3), 918–925 (2010).
[3]C. L. Eccles, L. A. Dawson, J. L. Moseley, and K. K. Brock, "Interfraction liver shape variability and impact on GTV position during liver stereotactic radiotherapy using abdominal compression," Int. J. Radiat. Oncol., Biol., Phys. **80**(3), 938–946 (2011).
[4]C. L. Eccles, R. Patel, A. K. Simeonov, G. Lockwood, M. Haider, and L. A. Dawson, "Comparison of liver tumor motion with and without abdominal compression using cine-magnetic resonance imaging," Int. J. Radiat. Oncol., Biol., Phys. **79**(2), 602–608 (2011).
[5]K. P. Tiev, S. Rivière, T. Hua-Huy, J. Cabane, and A. T. Dinh-Xuan, "Respiratory motion reduction in PET/CT using abdominal compression for lung cancer patients," PLoS One **9**(5), e98033 (2014).
[6]R. A. Siochi, Y. Kim, and S. Bhatia, "Tumor control probability reduction in gated radiotherapy of non-small cell lung cancers: A feasibility study," J. Appl. Clin. Med. Phys. **16**(1), 4444 (11pp.) (2014).
[7]S. A. Yoganathan, K. J. Das, D. G. Raj, and S. Kumar, "Dosimetric verification of gated delivery of electron beams using a 2D ion chamber array," J. Med. Phys. **40**(2), 68–73 (2015).
[8]P. Freislederer, M. Reiner, W. Hoischen, A. Quanz, C. Heinz, F. Walter, C. Belka, and M. Soehn, "Characteristics of gated treatment using an optical surface imaging and gating system on an Elekta linac," Radiat. Oncol. **10**, 68 (6pp.) (2015).
[9]E. Weiss, S. P. Robertson, N. Mukhopadhyay, and G. D. Hugo, "Tumor, lymph node, and lymph node-to-tumor displacements over a radiotherapy series: Analysis of interfraction and intrafraction variations using active breathing control (ABC) in lung cancer," Int. J. Radiat. Oncol., Biol., Phys. **82**(4), e639–e645 (2012).
[10]K. E. Mittauer, R. Deraniyagala, J. G. Li, B. Lu, C. Liu, S. S. Samant, J. L. Lightsey, and G. Yan, "Monitoring ABC-assisted deep inspiration breath hold for left-sided breast radiotherapy with an optical tracking system," Med. Phys. **42**(1), 134–143 (2015).
[11]A. N. Gutiérrez, S. Stathakis, R. Crownover, C. Esquivel, C. Shi, and N. Papanikolaou, "Clinical evaluation of an immbolization system for stereotactic body radiotherapy using helical tomotherapy," Med. Dosim. **36**(2), 126–129 (2011).
[12]J. H. Heinzerling, J. F. Anderson, L. Papiez, T. Boike, S. Chien, G. Zhang, R. Abdulrahman, and R. Timmerman, "Four-dimensional computed tomography scan analysis of tumor and organ motion at varying levels of abdominal compression during stereotactic treatment of lung and liver," Int. J. Radiat. Oncol., Biol., Phys. **70**(5), 1571–1578 (2008).
[13]G. Bouilhol, M. Ayadi, S. Rit, S. Thengumpallil, J. Schaerer, J. Vandemeulebroucke, L. Claude, and D. Sarrut, "Is abdominal compression useful in lung stereotactic body radiation therapy? A 4DCT and dosimetric lobe-dependent study," Phys. Med. **29**(4), 333–340 (2013).
[14]M. Xi, M. Z. Liu, L. Zhang, Q. Q. Li, X. Y. Huang, H. Liu, and Y. H. Hu, "How many sets of 4DCT images are sufficient to determine internal target volume for liver radiotherapy?," Radiother. Oncol. **92**(2), 255–259 (2009).
[15]J. Liu, J. Z. Wang, J. D. Zhao, Z. Y. Xu, and G. L. Jiang, "Use of combined maximum and minimum intensity projections to determine internal target volume in 4-dimensional CT scans for hepatic malignancies," Radiat. Oncol. **7**, 11 (8pp.) (2012).
[16]G. Gong, Y. Yin, L. Xing, Y. Guo, J. Chen, T. Liu, J. Lu, C. Ma, T. Sun, T. Bai, G. Zhang, and W. Deng, "Comparison of internal target volumes for hepatocellular carcinoma defined using 3DCT with active breathing coordinator and 4DCT," Technol. Cancer Res. Treat. **10**(6), 601–606 (2011).
[17]M. Xi, M. Z. Liu, X. W. Deng, L. Zhang, X. Y. Huang, H. Liu, Q. Q. Li, Y. H. Hu, L. Cai, and N. J. Cui, "Defining internal target volume (ITV) for hepatocellular carcinoma using four-dimensional CT," Radiother. Oncol. **84**(3), 272–278 (2007).
[18]Y. Akino, R. J. Oh, N. Masai, H. Shiomi, and T. Inoue, "Evaluation of potential internal target volume of liver tumors using cine-MRI," Med. Phys. **41**(11), 111704 (8pp.) (2014).
[19]K. Sheng, S. Gou, J. Wu, and S. X. Qi, "Denoised and texture enhanced MVCT to improve soft tissue conspicuity," Med. Phys. **41**(10), 101916 (10pp.) (2014).
[20]R. L. Baron, "Understanding and optimizing use of contrast material for CT of the liver," AJR, Am. J. Roentgenol. **163**, 323–331 (1994).
[21]A. S. Beddar, T. M. Briere, P. Balter, T. Pan, N. Tolani, C. Ng, J. Szklaruk, and S. Krishnan, "4D-CT imaging with synchronized intravenous contrast

injection to improve delineation of liver tumors for treatment planning," Radiother. Oncol. **87**(3), 445–448 (2008).
[22]M. W. Kissick, S. A. Boswell, R. Jeraj, and T. R. Mackie, "Confirmation, refinement, and extension of a study in intrafraction motion interplay with sliding jaw motion," Med. Phys. **32**(7), 2346–2350 (2005).
[23]J. N. Yang, T. R. Mackie, P. Reckwerdt, J. O. Deasy, and B. R. Thomadsen, "An investigation of tomotherapy beam delivery," Med. Phys. **24**(3), 425–436 (1997).
[24]K. Dohmen, H. Tanaka, M. Haruno, and Y. Niho, "Hepatic hydrothorax occurring rapidly after manual abdominal compression," World J. Gastroenterol. **13**(46), 6284–6285 (2007).